

LA-UR-12-23278 (Accepted Manuscript)

Beam debunching due to ISR-induced energy diffusion

Yampolsky, Nikolai A. Carlsten, Bruce E.

Provided by the author(s) and the Los Alamos National Laboratory (2017-09-20).

To be published in: Nuclear Instruments and Methods in Physics Research Section A: Accelerators,

Spectrometers, Detectors and Associated Equipment

DOI to publisher's version: 10.1016/j.nima.2017.06.023

Permalink to record: http://permalink.lanl.gov/object/view?what=info:lanl-repo/lareport/LA-UR-12-23278

Disclaimer

Approved for public release. Los Alamos National Laboratory, an affirmative action/equal opportunity employer, is operated by the Los Alamos National Security, LLC for the National Nuclear Security Administration of the U.S. Department of Energy under contract DE-AC52-06NA25396. Los Alamos National Laboratory strongly supports academic freedom and a researcher's right to publish; as an institution, however, the Laboratory does not endorse the viewpoint of a publication or guarantee its technical correctness.



Accepted Manuscript

Beam debunching due to ISR-induced energy diffusion

Nikolai Yampolsky, Bruce E. Carlsten

PII: S0168-9002(17)30676-9

DOI: http://dx.doi.org/10.1016/j.nima.2017.06.023

Reference: NIMA 59914

To appear in: Nuclear Inst. and Methods in Physics Research, A

Received date: 6 April 2017 Revised date: 13 June 2017 Accepted date: 14 June 2017



Please cite this article as: N. Yampolsky, B.E. Carlsten, Beam debunching due to ISR-induced energy diffusion, *Nuclear Inst. and Methods in Physics Research*, A (2017), http://dx.doi.org/10.1016/j.nima.2017.06.023

This is a PDF file of an unedited manuscript that has been accepted for publication. As a service to our customers we are providing this early version of the manuscript. The manuscript will undergo copyediting, typesetting, and review of the resulting proof before it is published in its final form. Please note that during the production process errors may be discovered which could affect the content, and all legal disclaimers that apply to the journal pertain.

Beam debunching due to ISR-induced energy diffusion

Nikolai Yampolsky and Bruce E. Carlsten

Los Alamos National Laboratory, Los Alamos, New Mexico, 87545, USA

Abstract

One of the options for increasing longitudinal coherency of X-ray free electron lasers (XFELs) is seeding with a microbunched electron beam. Several schemes leading to significant amplitude of the beam bunching at X-ray wavelengths were recently proposed. All these schemes rely on beam optics having several magnetic dipoles. While the beam passes through a dipole, its energy spread increases due to quantum effects of synchrotron radiation. As a result, the bunching factor at small wavelengths reduces since electrons having different energies follow different trajectories in the bend. We rigorously calculate the reduction in the bunching factor due to incoherent synchrotron the radiation while the beam travels in an arbitrary beamline. We apply general results to estimate reduction of harmonic current in common schemes proposed for XFEL seeding.

Keywords: Beam dynamics, synchrotron radiation, free electron lasers, seeding schemes

PACS: 41.60.Ap, 41.85.Ja, 42.50.Wk, 41.60.Cr, 52.59.Wd

1. Introduction

Free electron lasers (FELs) can be scaled to generate narrowband radiation in a wide frequency range. Currently existing FELs cover bandwidths from THz to hard X-rays. A conventional method for decreasing the FEL bandwidth is done by placing the undulator inside the optical cavity. However, this approach fails for X-ray FELs (XFELs) due to lack of high quality reflecting mirrors at these frequencies. As a result, modern XFELs typically operate in a single pass self-amplified spontaneous emission (SASE) regime in which broadband shot noise due to discreetness of the electron beam is amplified within the FEL bandwidth [1]. The bandwidth of these XFELs

can be reduced by seeding them with a narrowband signal rather than white noise.

A growing FEL mode couples radiation with particle motion. Therefore, an XFEL can be seeded either with narrowband radiation [2, 3] or with an electron beam modulated at the X-ray wavelength [4]. The second option looks attractive since electrons are charged particles and they can interact with electromagnetic fields unlike radiation which only weakly interacts with materials at X-ray frequencies. Several schemes predicting significant bunching at high harmonics for available coherent light sources were recently proposed [5, 6, 7]. All these schemes utilize magnetic bends for manipulating a modulated electron bunch. Electrons passing through bends emit synchrotron radiation. At high energies electrons emit radiation at high frequencies and quantum effects should be included to find the correct electron energy loss. Incoherent synchrotron radiation (ISR) has a nearly 100% frequency spread which results in electron energy diffusion when quantum effects are accounted for since the electron energy loss can be described by a random walk model. Electron energy diffusion translates into diffusion in longitudinal position since bends are dispersive elements (electrons with different energies travel along different trajectories). As a result, a prebunched electron beam smears out when it passes through bends and the bunching factor reduces.

The effect of the beam debunching becomes stronger for FELs seeded at smaller wavelengths. First of all, an energetic electron bunch is required to generate short wavelength FEL radiation which increases ISR-induced energy diffusion in the beamline bends. At the same time, even a small longitudinal spread could cause significant debunching at a shorter wavelength modulation. These two effects combined result in stronger smearing of harmonic current for short wavelength XFELs. Therefore, there is a physical limit on the shortest wavelength bunching which can be created in various schemes for generating high harmonic content. This effect was estimated for various XFEL seeding schemes [5, 8, 9] but those estimates were qualitative or numerical and did not include detailed trade-off studies. It is the purpose of this paper to study this effect rigorously and find accurate quantitative estimates of the degradation of harmonic current in various beamline configurations.

2. Qualitative estimate for smearing of harmonic current

First, we estimate the parameter region in which smearing of harmonic current due to ISR-induced energy spread is significant. We consider the last dipole of some beamline optics which leads to longitudinal bunching from an imposed energy modulation. The argument bellow is valid for any such seeding scheme.

Quantum effects in ISR at high energies result in energy diffusion as described in Ref. [10]

$$\langle \Delta E^2 \rangle = 2Ds, \quad D = \frac{55}{48\sqrt{3}} \frac{\hbar e^2 c}{\rho^3} \gamma^7,$$
 (1)

where D is the energy diffusion coefficient, $\rho = \beta \gamma mc/(eB)$ is the electron gyroradius in the magnetic field B; \hbar is the reduced Planck constant, and s is the path length. Two identical electrons entering the dipole exit at different longitudinal positions since their energies become different inside the dipole due to ISR and the dipole energy dispersion transforms this energy difference into different longitudinal positions. As a result, a bunched beam smears out. We approximate this effect assuming energies of two electrons to be constant along the bend but to be different by the overall induced energy spread due to ISR, $\Delta E = \sqrt{2Ds}$. The path length of an electron inside the magnet of length L is equal to

$$s = \rho \arcsin \frac{L}{\rho}.$$
 (2)

Then the path difference of electrons having different energies is

$$\Delta s = \frac{\partial s}{\partial \rho} \frac{\partial \rho}{\partial E} \Delta E \approx -\frac{L}{3} \alpha^2 \frac{\Delta E}{E},\tag{3}$$

where α is the bend angle of the test electron inside the bend.

This path difference results in smearing of the imposed modulation. Smearing is significant if the path difference is on the order of a half wavelength of the modulation. Then one obtains the qualitative estimate for parameters region in which ISR-induced debunching is not significant.

$$\frac{55}{54\sqrt{3}} \frac{\hbar e^2}{m^2 c^3} \frac{\alpha^7 \gamma^5}{\lambda^2} = 90.6 \frac{\alpha^7 [\text{deg}]}{\lambda^2 [\mathring{A}]} \left(\frac{E}{10 GeV}\right)^5 \ll 1.$$
 (4)

This estimate shows that beam bunching for hard X-ray FELs ($\lambda \sim 1\,\text{Å}$, $E \sim 10 \text{GeV}$) requires the use of optical elements with weak bends having sub-degree bend angles. However, this estimate does not predict how fast the bunching degrades along the bend. In particular, it is not clear how fast the bunching drops to zero and how far one can go beyond this limit without dramatic loss in bunching amplitude.

3. Smearing of harmonic current in arbitrary beamline

3.1. Vlasov equation

Any electron beam can be described as an ensemble of electrons occupying some phase space volume. This ensemble can be described by the phase space distribution function $f(\zeta)$, where ζ is the 6D phase space coordinate of each electron

$$\boldsymbol{\zeta} = (x, p_x, y, p_y, \Delta t, -\Delta E), \tag{5}$$

where x and y are the transverse electron coordinates in respect to the reference trajectory, p_x and p_y are the corresponding momenta, Δt is the deviation of arrival time to position s along the beamline, and ΔE is the deviation of particle energy from the average bunch energy.

The bunch interacts with electro-magnetic fields while it travels along the beamline. These forces satisfy Maxwell equations which indicates that beam dynamics is Hamiltonian and it is fully described by a Hamiltonian $H(\zeta, s)$. The evolution of the distribution function satisfies Vlasov equation which can be considered as a continuity equation in phase space

$$\frac{df}{ds} = \partial_s f(\boldsymbol{\zeta}, s) + \{f, H\} = \partial_s f + (\nabla f)^T J(\nabla H) = 0, \tag{6}$$

where $\{f, H\} = (\nabla f)^T J(\nabla H)$ is the Poison bracket, J is the unit block-diagonal antisymmetric symplectic matrix, ∇ is the 6D gradient in the phase space, and superscript T stands for transposition.

Typically the electron bunch can be considered well localized and quasimonoenergetic. Under this assumption, forces can be well approximated by a linear function in respect to their phase space coordinates. The corresponding Hamiltonian describing beam dynamics is quadratic then, $H(\zeta, s) =$ $1/2\zeta^T\mathcal{H}(s)\zeta$, $\mathcal{H} = \mathcal{H}^T$. The trajectory of each electron defines the map in the phase space which can be described with the transform matrix $R(s, s_0)$

for linear beamlines. Then the formal solution for the Vlasov equation (6) can be presented in the following form

$$f(\boldsymbol{\zeta}, s) = f(R^{-1}(s, s_0)\boldsymbol{\zeta}, s_0), \qquad (7)$$

$$f(\boldsymbol{\zeta}, s) = f\left(R^{-1}(s, s_0)\boldsymbol{\zeta}, s_0\right),$$

$$\frac{dR(s, s_0)}{ds} = J\mathcal{H}R(s, s_0),$$

$$R(s_0, s_0) = I.$$
(8)

Alternatively, the dynamics of modulated beams can be conveniently described in the spectral domain as illustrated in Ref. [11]. This representation is particularly useful for the description of modulated beams since they are well localized in the spectral domain for quasi-monochromatic modulations. For linear optics, the beam can be fully described by the Hamiltonian evolution of its 6D spectral distribution which evolution as

$$f_{\mathbf{k}}(\mathbf{k}, s) = \int f(\boldsymbol{\zeta}, s) e^{i\mathbf{k}^T \boldsymbol{\zeta}} d^6 \boldsymbol{\zeta}, \tag{9}$$

$$\frac{df_{\mathbf{k}}}{ds} = \frac{\partial f_{\mathbf{k}}}{ds} + \{f_{\mathbf{k}}, H_{\mathbf{k}}\} = 0, \quad H_{\mathbf{k}} = -\frac{1}{2}\mathbf{k}^T J \mathcal{H} J \mathbf{k}.$$
 (10)

The solution of the spectral Vlasov equation was found in Ref. [11]

$$f_{\mathbf{k}}(\mathbf{k}, s_0) = f_{\mathbf{k}}(R^T(s, s_0)\mathbf{k}, s_0). \tag{11}$$

This solution indicates that the spectral distribution function remains constant along characteristics in the spectral domain

$$\mathbf{k}(s) = R^{-T}(s, s_0)\mathbf{k}(s_0), \tag{12}$$

which reduces the evolution of each spectral component to a linear transform of its modulation wavevector.

3.2. Boltzmann equation in phase space domain

Synchrotron radiation of highly relativistic electrons is confined within a small angle with respect to the electron instantaneous velocity, $\Delta\theta \sim 1/\gamma \ll$ 1. Therefore, emission of a photon with angular frequency ω mainly results in the reduction of the electron energy by $\Delta E = \hbar \omega$. The change of the electron transverse momenta is on the order of $1/\gamma$ smaller then the change of the longitudinal momentum and can be ignored to the first order. Assuming that the emission process is instantaneous in time, one can use the Vlasov equation (6) to describe the electron dynamics between photon emission events.

Electron energy loss due to photon emission results in a collision operator which changes the density in phase space. A large number of electrons within the bunch and the ergodicity property allows one to reduce discrete emission events to a continuous change of the ensemble distribution. As a result, the evolution of an electron bunch can be described with the following Boltzmann equation

$$\frac{df}{ds} = \partial_s f + \{f, H\} = C^{ISR}[f], \tag{13}$$

$$C^{\text{ISR}}[f] = \int_{0}^{\infty} f(E + \hbar\omega) \frac{dN(\omega, E + \hbar\omega)}{d\omega} d\omega -$$

$$- \int_{0}^{\infty} f(E) \frac{dN(\omega, E)}{d\omega} d\omega,$$
(14)

where $C^{\rm ISR}[f]$ is the collision operator for ISR energy loss which describes the detailed balance between electron states. H is the beamline Hamiltonian if synchrotron radiation is neglected, $(dN/d\omega)d\omega ds$ is the probability for a photon emission within bandwidth $d\omega$ while electron travels distance ds. The probability of photon emission is related to the power spectrum $dP/d\omega$ of a single electron synchrotron radiation [12]

$$\frac{dN}{d\omega} = \frac{1}{\hbar\omega} \frac{dP}{d\omega} = \frac{1}{\hbar\omega} \frac{\sqrt{3}e^2}{2\pi\rho c} \gamma \frac{\omega}{\omega_c} \int_{\omega/\omega_c}^{\infty} K_{5/3}(x) dx, \tag{15}$$

$$\omega_c = \frac{3}{2} \frac{\gamma^3 c}{\rho}.\tag{16}$$

Note that collision operator $C^{\rm ISR}[f]$ describing ISR-induced energy losses is linear with respect to the electron distribution function. This property reflects the fact that ISR is a single particle effect. Superposition of radiation fields from many particles and the influence of the resulting Coherent Synchrotron Radiation (CSR) force on particle dynamics is not included in this model. The presented model also assumes that photons do not interact with other electrons once they are emitted.

The Boltzmann equation described by Eq. (13) can be used to determine the main parameters of ISR. For example, one can easily find the overall

energy loss and the energy diffusion

$$\left(\frac{d\langle E\rangle}{ds}\right)_{\text{ISR}} = \int EC^{\text{ISR}}[f]d^6\zeta = -P, \tag{17}$$

$$\left(\frac{d\langle \Delta E^2 \rangle}{ds}\right)_{\text{ISR}} = \int (E - \langle E \rangle)^2 C^{\text{ISR}}[f] d^6 \zeta = 2D, \tag{18}$$

where $\langle E \rangle = \int E f d^6 \zeta$ is the mean electron energy and $\langle \Delta E^2 \rangle = \int (E - \langle E \rangle)^2 f d^6 \zeta$ is the rms energy spread. These coefficients can be expressed through the synchrotron radiation power spectrum.

$$P = \int_{0}^{\infty} \frac{dP}{d\omega} d\omega = \frac{2}{3} \frac{e^2}{\rho^2} \gamma^4, \tag{19}$$

$$D = \frac{1}{2} \int_{0}^{\infty} \hbar \omega \frac{dP}{d\omega} d\omega = \frac{55}{48\sqrt{3}} \frac{\hbar e^2 c}{\rho^3} \gamma^7.$$
 (20)

Note that the overall change of beam energy and energy spread are described with Eqns. (17) and (18) if the beam is not accelerated and the beamline does not contain elements having nonzero R_{6i} beam matrix elements (where i = 1, ..., 6), e.g high order mode RF cavities introducing energy slews.

3.3. Boltzmann equation and its solution in spectral domain

The Boltzmann equation described with Eq. (13) — (14) is a complicated integro-differential equation. On the other hand, this equation takes a much simpler form in the spectral domain. The appropriate equation can be found by taking the Fourier transform of the Boltzmann equation (13). Its left-hand side is the same as the Vlasov equation (6) and, therefore, its Fourier transform reduces to the spectral Vlasov equation (10). The Fourier transform of the ISR collision operator results in the corresponding collision operator in the spectral domain. One can find it to be equal to

$$C_{\mathbf{k}}^{\mathrm{ISR}} = \int f(\zeta) e^{-i\mathbf{k}^{T}\zeta} \int_{0}^{\infty} (e^{ik_{E}\hbar\omega} - 1) \frac{dN}{d\omega} d\omega d^{6}\zeta.$$
 (21)

where k_E is the component of the modulation wavevector **k** along the energy coordinate.

These integrals can be evaluated under assumption that the electron bunch is quasi-monoenergetic. In this case, the ISR spectrum can be assumed to be the same for all the particles and the integral over photon frequency can be evaluated independently from the integral over the phase space and yields the spectral distribution function. This assumption is equivalent to neglecting the radiation cooling effect which is a valid approximation for high brightness linear machines.

The integral over photon frequencies can be evaluated using the spectral distribution of the ISR power (15) and then the spectral Boltzmann equation takes the following form

$$\frac{df_{\mathbf{k}}}{ds} = \frac{\partial f_{\mathbf{k}}}{ds} + \{f_{\mathbf{k}}, H_{\mathbf{k}}\} = C_{\mathbf{k}}^{\text{ISR}},$$

$$C_{\mathbf{k}}^{\text{ISR}} = (-ik_{E}P^{\text{eff}} - k_{E}^{2}D^{\text{eff}})f_{\mathbf{k}},$$
(22)

$$C_{\mathbf{k}}^{\text{ISR}} = (-ik_E P^{\text{eff}} - k_E^2 D^{\text{eff}}) f_{\mathbf{k}}, \tag{23}$$

$$P^{\text{eff}}(\varkappa) = \frac{54}{55} \frac{5\varkappa\sqrt{1+\varkappa^2} - 3\sinh(\frac{5}{3}\sinh(\varkappa))}{\varkappa^3\sqrt{1+\varkappa^2}} P, \qquad (24)$$

$$D^{\text{eff}}(\varkappa) = \frac{9}{8} \frac{-\sqrt{1+\varkappa^2} + \cosh(\frac{5}{3}\sinh(\varkappa))}{\varkappa^2\sqrt{1+\varkappa^2}} D, \qquad (25)$$

$$D^{\text{eff}}(\varkappa) = \frac{9}{8} \frac{-\sqrt{1+\varkappa^2} + \cosh(\frac{5}{3}\sinh(\varkappa))}{\varkappa^2\sqrt{1+\varkappa^2}} D, \tag{25}$$

$$\varkappa = k_E \hbar \omega_c, \tag{26}$$

One can note that the Boltzmann equation (22) — (23) in the spectral domain has much simpler form compared to the Boltzmann equation in the phase space domain (13) — (14). The ISR collision operator in the spectral domain $C_{\mathbf{k}}^{\text{ISR}}$ algebraically depends on the spectral distribution function which indicates that different spectral components evolve independently from each other. The collision operator depends on two parameters, namely the effective energy loss P^{eff} and diffusion D^{eff} coefficients, as described by Eqs. (24) — (26). The effective energy loss term results in the change of each spectral component phase which corresponds to the loss of the mean bunch energy while the absolute amplitude of each component is not affected. However, the effective energy diffusion term results in the reduction of each spectral component amplitude which manifests as smearing of the associated harmonic current in the phase space domain.

The effective energy loss and diffusion parameters depend on a single parameter $\varkappa = k_E \hbar \omega_c$. The nonzero energy modulation wavenumber k_E indicates presence of energy bands in the phase space distribution separated by $\Delta E_{bands} = 2\pi/k_E$. Electrons passing through the bend emit photons which reduce the electron energy by $\Delta E_{\rm ISR} = \hbar \omega$ in a single emission event.

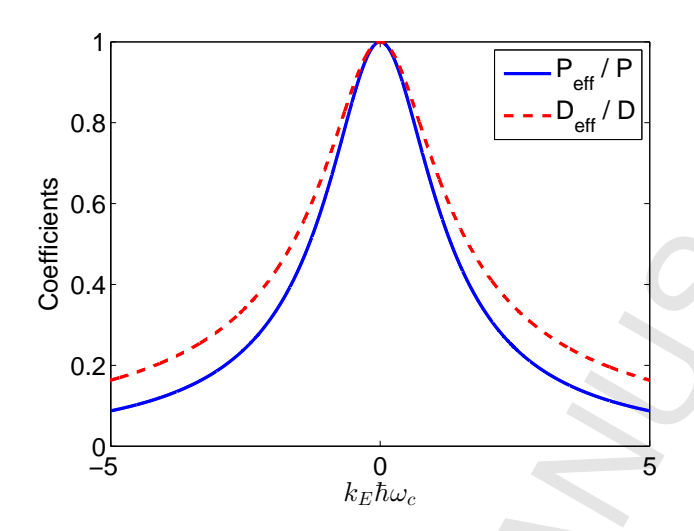


Figure 1: (Color online) Dependence of effective energy loss P^{eff} and diffusion D^{eff} coefficients on $k_E\hbar\omega_c$.

If all electrons would lose the same energy in a single photon emission event $\langle \Delta E_{\rm ISR} \rangle = \hbar \omega_c$ then the distribution function would not change if $\langle \Delta E_{\rm ISR} \rangle = \Delta E_{bands}$ since all the electrons would move into the same position within the next band and all the bands are equally populated. Then the energy diffusion would vanish at $k_E \hbar \omega_c = 2\pi$ in this hypothetical scenario. However, photons emitted due to ISR have nearly 100% frequency distribution, so in reality electrons do not move into the same position within the next energy band but also acquire some random misplacement which is manifested as energy diffusion. At the same time, the diffusion coefficient at $\varkappa = 2\pi$ is much smaller compared to the case of $\varkappa \ll 1$ (as illustrated in Fig. 1) since a large fraction of electrons do not significantly change their relative positions within the corresponding band.

The Boltzmann equation in the spectral domain is a linear hyperbolic equation which can be solved using method of characteristics. The characteristics describing trajectories in the spectral domain are the same as for the Vlasov equation (12). This property indicates that the transform of the modulation wavevector is independent whether ISR is accounted for or not. Taking ISR into account (both overall energy loss and energy diffusion) results in a change of the harmonic current amplitude and phase along the beamline. Note that the optics required to transform an initial modulation into a designed microbunched beam, including the bunching wavelength, are

not affected by ISR. This property is highly useful in studies of XFEL seeding schemes since the beamline optics can be designed without accounting for ISR, which can then be included at the last stage for estimating the reduction of the final bunching factor.

The absolute amplitude of the spectral distribution changes due to the effective energy diffusion effect but it is not affected by the overall energy loss. One can find the solution of linear Eqs. (22) — (23) in the following form which can be used to find the smearing of the harmonic current due to ISR in any arbitrary linear beamline

$$\left| \frac{f_{\mathbf{k}}(\mathbf{k}(s_f), s_f)}{f_{\mathbf{k}}(\mathbf{k}(s_0), s_0)} \right| = \exp\left(- \int_{s_0}^{s_f} k_E^2(s) D^{\text{eff}}(s) ds \right), \tag{27}$$

$$\mathbf{k}(s) = R^{-T}(s, s_0)\mathbf{k}(s_0). \tag{28}$$

There are several properties which follow from Eq. (27). First of all, the harmonic current amplitude always reduces along the beamline. This property reflects the diffusive nature of ISR which smears out small scale variations in the distribution function. Another property states that the rate of modulation smearing is proportional to k_E^2 . This property reflects the fact that ISR-induced diffusion is the energy diffusion. A uniform energy distribution is not affected by this effect. Also note that the integral along the beamline in Eq. (27) can be substituted as a sum of integrals along each element. Importantly, as a result, the overall attenuation of the harmonic current is equal to the product of attenuations in each dipole.

3.4. Fokker-Planck approximation

The Boltzmann equation in the phase space domain (13) — (14) can be simplified under the assumption that the characteristic energy scale of the distribution function $f/\partial_E f$ is much larger than the characteristic energy $\hbar\omega_c$ of the emitted photons. Then the distribution function in the collision operator (14) can be expanded and the following Fokker-Planck equation recovered

$$\frac{df}{ds} = \partial_E(Pf) + \partial_{EE}^2(Df), \tag{29}$$

where energy loss P and diffusion D coefficients are described by Eqns. (17) and (18).

The Fokker-Planck equation can be solved in the spectral domain in the same way as was done in Sec. 3.3 for the Boltzmann equation. However, this

analysis is not required since the Fokker-Planck equation is an approximation of a more general Boltzmann equation and its solution can be recovered from a general solution. The Boltzmann equation (13) yields the Fokker-Planck approximation when the typical energy of the emitted photons is much smaller than the characteristic energy scale of the electron distribution function. This assumption corresponds to the limit of $k_E\hbar\omega_c\ll 1$ as discussed in Sec. 3.3. Therefore, the solution of the Fokker-Planck equation (29) can be found as a small photon energy limit of the general solution for the Boltzmann equation (27), when $D^{\rm eff}=D$.

The smearing of the harmonic current depends on the energy modulation wavenumber along the beamline which can be found using the transform (28). Consider, for example, some beamline for XFEL seeding scheme. As discussed in Ref. [11] such a beamline is designed to recover an imposed modulation as longitudinal bunching at a given wavenumber, $\mathbf{k}(s_f) = \hat{\mathbf{k}}_z k = (0,0,0,0,k,0)^T$. Then the modulation wavevector at any given position along the beamline can be expressed through the modulation wavevector at the final position and the linear transform matrix as $\mathbf{k}(s) = R^T(s_f, s)\mathbf{k}(s_f)$. Then one can find that the overall attenuation of harmonic current due to ISR-induced energy spread in the Fokker-Planck approximation is equal to

$$A \equiv \left| \frac{f_{\mathbf{k}}(\mathbf{k}(s_f), s_f)}{f_{\mathbf{k}}(\mathbf{k}(s_0), s_0)} \right| = \exp\left(-k^2 \int_{s_0}^{s_f} DR_{56}^2(s_f, s) ds\right)$$
(30)

This result agrees with qualitative estimate presented in Ref. [9]. The solution shows that the degradation of harmonic current strongly increases in beamlines having large energy dispersion. Therefore, conventional XFEL seeding schemes utilizing chicanes [4, 6, 5] might be affected by ISR since chicanes are specifically designed to have large energy dispersion R_{56} .

4. Smearing of bunching in various XFEL seeding schemes

In this section we calculate the attenuation of the harmonic current in various beamlines designed for seeding XFELs with microbunched electron beams. In these schemes the beam is typically modulated in an undulator by interacting with an external laser at a resonant wavelength and longitudinal bunching at high harmonics is recovered in the following linear beamline. This dynamics can be conveniently described in the spectral domain as was

illustrated in Ref. [11]. This formalism describes the change of the spectral distribution function along characteristics which can be considered as trajectories of the modulation wavevector in the spectral domain. The trajectory of each spectral component does not depend whether ISR energy diffusion is neglected or taken into account which follows from Eq. (28) since it is independent on the diffusion coefficient. Taking into account ISR-induced energy diffusion manifests as a next order effect and results in the reduction of the harmonic current along the beamline. The exponential factors in Eqs. (27) and (30) can be interpreted as attenuation of harmonic current due to ISR-induced energy diffusion.

In our analysis we limit ourselves to modulations which are recovered as longitudinal bunching at a designed wavelength at the end of a chosen beamline element. Then the beam modulation at the beginning of the beamline element is well defined since its transform is described by Eq. (28). From this perspective, the precise mechanism of imposing initial modulation is not important. Therefore, the attenuation factor for each element will depend on the output bunching wavelength and beamline parameters.

We will present estimates for the attenuation factor based on the the solution of the Fokker-Planck equation described by Eq. (30) since it is much simpler than the solution of the Boltzmann equation (27) and the integrals can be calculated analytically. This approximation is valid when the condition $k_E\hbar\omega_c\ll 1$ is held. The energy wavenumber of modulation can be expressed through the wavelength of the final longitudinal bunching and the beamline dispersion. In this section we will use conventional units used in beam physics, particularly we will use the relative energy spread instead of the full energy deviation, $\Delta E = \gamma mc^2(\Delta\gamma/\gamma)$. Then the condition for validity of the Fokker-Planck equation expressed in common units reads as

$$(R_{56}(s_f, s))_{\text{max}} \ll \frac{2\lambda\rho}{3\lambda_e\gamma^2} = 2.39 \frac{\lambda[\mathring{A}]}{B[T]} \frac{10GeV}{E} \mu m, \tag{31}$$

where λ is the output bunching wavelength and $\lambda_e = 2\pi\hbar/(mc) \approx 2.43 \cdot 10^{-12} m$ is Compton wavelength.

4.1. Single bend

First, we estimate the attenuation of the harmonic current in a single bend which can be the last bend of a more complicated linear beamline. The transform matrix of a bend is described with Eq. (A.10). Then the

attenuation of the harmonic current can be found from Eq. (30) and for a single bend it is equal to

$$A_{\text{bend}} = \exp\left(-k^2 \frac{D}{c} \int_0^\alpha R_{56}^2(\theta) d(\rho \theta)\right) =$$

$$= \exp\left(-\frac{55\pi^2}{63 \cdot 48\sqrt{3}} \frac{\alpha^7 \gamma^5}{\alpha_{fine}} \left(\frac{r_e}{\lambda}\right)^2\right) \approx$$

$$\approx \exp\left(-16 \left(\frac{E}{10 \text{GeV}}\right)^5 \frac{\alpha^7 [deg]}{\lambda^2 [\mathring{A}]}\right), \tag{32}$$

where α is the dipole bend angle, $\alpha_{fine}=e^2/(\hbar c)\approx 1/137$ is the fine structure constant, and $r_e=e^2/(mc^2)\approx 2.818\cdot 10^{-15}m$ is the classical electron radius.

The smearing of the harmonic current can be neglected if the exponent argument is smaller than unity. That results in a maximum angle of the bend which can be used in the beamline. Exceeding this critical value results in a strong smearing of the harmonic current due to the very strong scaling of attenuation with the bend angle. The parameter region of importance of the ISR debunching agrees with the qualitative estimate (4). The qualitative estimate shows the same scaling versus main beam parameters as in the rigorous analysis but the numerical factor is about a factor of 6 larger since the ISR-induced energy spread was assumed to be acquired in the beginning of the bend rather than being uniformly distributed along its length.

4.2. Chicane

Most of the beam-based XFEL seeding schemes utilize chicanes [4, 6, 5, 7]. To estimate the effect of ISR in these schemes we consider that the chicane is designed to transform an imposed space-energy modulation into a final longitudinal bunching. The detailed analysis of this setup is presented in Appendix A and it yields to the attenuation factor of

$$A_{\rm ch} = \exp\left\{-6700 \frac{\alpha^7 [\deg]}{\lambda^2 [\mathring{A}]} \left(\frac{E}{10 GeV}\right)^5 \times \left[\left(\frac{R_{56}}{\rho \alpha^3} + 0.072\right)^2 + 0.022\right]\right\}.$$
(33)

One can note that attenuation of harmonic current is stronger for larger chicanes. This result follows directly from the general expression (30) for

the attenuation factor in a general beamline. Typically, the chicane strength scales as $R_{56} \sim \rho \alpha^3$. Then this term becomes dominant compared to other numerical factors and the following approximate expression for attenuation can be used most of the time:

$$A_{\rm ch} \approx \exp\left\{-\frac{\alpha[\deg]R_{56}^2[\mu m]B^2[T]}{4.7\lambda^2[\mathring{A}]} \left(\frac{E}{10GeV}\right)^3\right\}. \tag{34}$$

This expression allows one to estimate the effect of ISR in proposed schemes for XFEL seeding with microbunched beam.

The High Gain Harmonic Generation (HGHG) scheme [4] uses a single modulator and a single chicane. The chicane strength required to achieve maximum bunching is approximately equal to $R_{56}(\Delta \gamma_{mod}/\gamma) = \mu_{n1}\lambda/2\pi$, where $\mu_{n1} \sim n$ is the first maximum of the n-th order Bessel function, $J'_n(\mu_{n1}) = 0$ [11]. Then the attenuation of the harmonic current in an HGHG scheme due to ISR can be estimated as

$$A_{HGHG} \approx \exp\left\{-5.4 \cdot 10^{-3} \mu_{n1}^2 \left(\frac{E}{10 GeV}\right)^3 \times \left(\frac{\Delta \gamma_{rms}}{\Delta \gamma_{mod}}\right)^2 \frac{\alpha [\deg] B^2 [T]}{(\Delta \gamma_{rms}/\gamma [0.01\%])^2}\right\}. \tag{35}$$

Note that the degradation of the harmonic current does not depend on the wavelength of the output bunching directly. It depends only on the harmonic number used in the HGHG scheme since $\mu_{n1} \sim n$ at $n \gg 1$.

Similar estimates can be made for harmonic current smearing in the Echo-Enabled Harmonic Generation (EEHG) scheme [5] and Compressed Harmonic Generation (CHG) scheme [6]. These schemes utilize two chicanes of different strengths, so the attenuation should be estimated for both chicanes. The first chicane in both schemes is used to create energy bands in the phase space from the modulation which can be considered as mostly longitudinal bunching, $k_E(s_f) \gg k_E(s_0)$. Therefore, the estimate (33) can be applied to the first chicane even though it was derived for a chicane which converts spatio-energetic modulation into purely longitudinal bunching. Straightforward algebra shows that the ratio of chicane strength and modulation wavelength is almost the same for both chicanes in EEHG and CHG schemes, $(R_{56}/\lambda)_{\text{chicane1}} \approx (R_{56}/\lambda)_{\text{chicane2}}$. Therefore, both chicanes in those schemes result in the same attenuation of harmonic current as if they

are designed using the same dipoles and the difference in their strengths is caused by different drift lengths within the doglegs. Then the attenuation of the harmonic current in an EEHG scheme can be estimated as

$$A_{EEHG} \approx \exp\left\{-10.8 \cdot 10^{-3} \mu_{n1}^2 \left(\frac{E}{10 GeV}\right)^3 \times \left(\frac{\Delta \gamma_{rms}}{\Delta \gamma_{mod2}}\right)^2 \frac{\alpha [\deg] B^2 [T]}{(\Delta \gamma_{rms}/\gamma [0.01\%])^2}\right\}, \tag{36}$$

where $\Delta \gamma_{mod2}$ is the energy modulation imposed in the second modulator. In this estimate we neglected the energy diffusion due to ISR in the second undulator which modulates the beam. This effect can be easily accounted for with the assumption that the undulator energy dispersion is much smaller as compared to that in the chicanes. Then the energy modulation wavenumber $k_E = \mu_{n1}/(\Delta \gamma_{mod2}/\gamma)$ is constant along the undulator and full attenuation factor for EEHG scheme should be reduced by $\exp(-k_E^2 D_{und} L)$, where L is the undulator length and D_{und} is the undulator energy diffusion coefficient found in Ref. [13] (the rms energy change by the undulator is $(\Delta \gamma/\gamma)^2 = 2D_{und}L$).

A similar estimate for a CHG seeding scheme yields

$$A_{CHG} \approx \exp\left\{-4.3 \cdot 10^7 (M+1)^2 \left(\frac{E}{10 GeV}\right)^3 \times \frac{\sigma_z^2 [\mu m]}{\lambda^2 [\mathring{A}]} \left(\frac{\Delta \gamma_{rms}}{\Delta \gamma_{ind}}\right)^2 \frac{\alpha [\deg] B^2 [T]}{(\Delta \gamma_{rms}/\gamma [0.01\%])^2}\right\},\tag{37}$$

where M is the compression factor in the CHG scheme and $\Delta \gamma_{ind}$ is the energy slew imposed on the beam inside the cavity (i.e. the additional energy at the location of the rms bunch length), and σ_z is the bunch length after compression. The estimate for smearing the harmonic current in a CHG scheme indicates that this effect is very strong compared to other seeding schemes. This result comes from the fact that chicanes used in a CHG are much stronger than what is required for HGHG and EEHG schemes. Chicanes in a CHG scheme need to change the relative particle positions on the order of the pulse length in order to provide significant compression, unlike harmonic generation schemes which require a change of the electron relative positions on the order of the modulation wavelength. Therefore,

a CHG scheme may be not feasible for seeding XFELs due to its inherent strong ISR-induced smearing of the harmonic current.

4.3. Emittance Exchanger

The smearing of the harmonic current is large in beamlines having a large energy dispersion R_{56} as discussed in Sec. 3.4. ISR-induced attenuation can be reduced by specifically designing beamline without energy dispersion. This approach implies that conventional schemes for XFEL seeding such as HGHG, EEHG, and CHG cannot be implemented since they rely on the presence of dispersive elements to recover imposed spatio-energetic modulation as longitudinal bunching. Therefore, one should consider imposing a modulation that is different from a modulation in E-z phase plane. For example, one can consider using Emittance EXchanger (EEX) optics [14] to transform transverse modulation into bunching [15, 7]. A properly designed EEX swaps the longitudinal and transverse phase spaces of the beam, and therefore, the energy dispersion of the beamline $R_{56}(s_f, s_0)$ is zero. However, the energy dispersion from the middle of the beamline to the end, $R_{56}(s_f, s)$, is not zero, and the attenuation of the harmonic current does not vanish in this setup as follows from Eq. (30). Additional minimization of the ISR-induced debunching can be achieved by using doglegs having zero dispersion so that energy modulation is kept small in the middle of the EEX optics. Zero energy dispersion of the dogleg can be achieved by inserting a quadrupoles triplet in the dogleg drifts so that the entire drift looks like an effective negative drift space in terms of linear transform matrix [16].

We design the following setup to recover longitudinal bunching using EEX optics. First, the beam is transversally modulated by passing it through a mask. Then the imposed modulation is recovered as longitudinal bunching with the following EEX optics. The dispersion of each dogleg is chosen to be zero to minimize ISR-induced smearing of harmonic current. Such a design requires that the beam is modulated along the x' phase space coordinate before the EEX optics. This can be achieved by inserting a focusing lens just in front of the EEX and placing the transverse mask in the focus plane of this lens as discussed in Ref. [16]. The attenuation of harmonic current in this scheme can be calculated using the same algorithm as discussed in Appendix Appendix A and one can find

$$A_{\text{EEX}} = \exp\left\{-390 \frac{\alpha^7 [\text{deg}]}{\lambda^2 [\mathring{A}]} \left(\frac{E}{10 GeV}\right)^5\right\}. \tag{38}$$

We numerically verify the quantitative estimate (38) by simulating the EEX optics with a simple particle pushing code. All the beamline elements were considered to be linear and the ISR was included as a random change of the electron energy at each time step within bends. The results are presented in Fig. 2 for the regime of $k_E\hbar\omega_c\ll 1$ in which the Fokker-Planck approximation can be used. The following parameters of the EEX optics were used: beam mean energy of E=12GeV and rms energy spread of $\Delta\gamma/\gamma=10^{-4}$, normalized transverse emittance $\epsilon_n=0.14$ mm-mrad, and beam sizes $\sigma_x=\sigma_y=\sigma_z=100\mu m$ in all dimensions The EEX transforms an initial transverse modulation with 23nm wavelength into 0.3Å longitudinal bunching. Using EEX dipoles with B=1T magnetic field and $\alpha=0.3$ degree angles. Fig. 2 shows perfect agreement between numerical simulations and quantitative analysis.

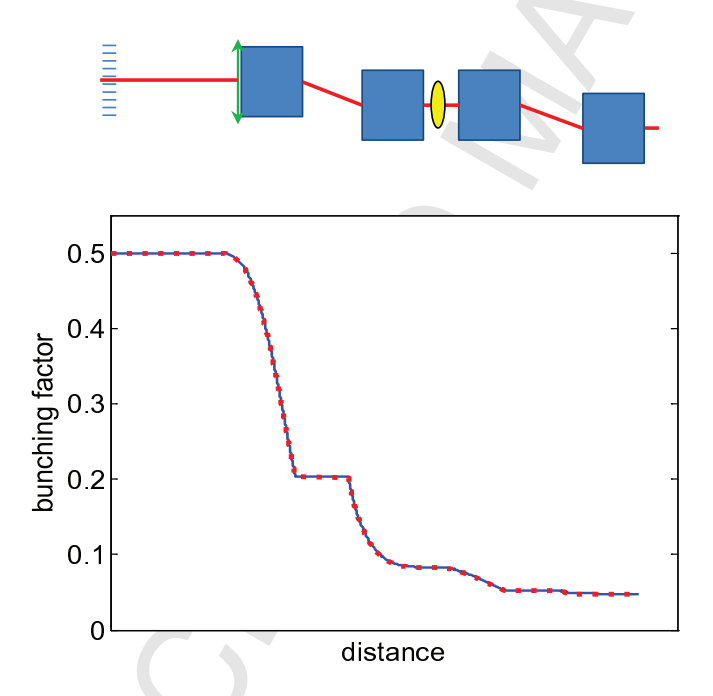


Figure 2: (Color online) Attenuation of harmonic current in EEX optics calculated numerically (solid blue line) and analytically (dotted red line).

Note that the attenuation of the harmonic current in the EEX optics described with Eq. (38) is similar to attenuation in a chicane having zero energy dispersion $R_{56} = 0$, as described by Eq. (33). This fact can be explained by the similarity of these two optics which require the same doglegs

having zero dispersion. Moreover, the scaling of the attenuation is the same for both schemes, $\ln A \propto -\alpha^7 \gamma^5 / \lambda^2$, but the corresponding numerical factors are different. The numerical factor for attenuation of harmonic current in the chicane is on the same order as for EEX if $R_{56} = 0$ and it is an order of magnitude larger compared to EEX if $R_{56} \sim \rho \alpha^3$. Also note that the same scaling holds for a single bend as described by Eq. (32).

5. Discussion

We developed a quantitative approach which allows one to calculate the smearing of the harmonic current due to ISR-induced energy spread in an arbitrary beamline. The approach is based on a beam representation in the spectral domain where modulation is represented as a well-localized distribution which evolves along the trajectories. The energy diffusion manifests in the spectral domain as a damping operator which allows one easily calculate attenuation of harmonic current amplitude along the beamline. The analysis can be further simplified using a Fokker-Planck approximation which is valid when the typical energy of emitted photons is much smaller than the energy bands of modulation.

We have applied the developed formalism to estimate the smearing of the harmonic current in various schemes proposed for seeding XFELs in which an imposed modulation is recovered as longitudinal bunching in following beamline. We demonstrated that the attenuation of the harmonic current amplitude increases in beamlines having large energy dispersion R_{56} . The different schemes lead to the same scaling for the attenuation of the harmonic current, $\ln A \propto -\alpha^7 \gamma^5 / \lambda^2$, which follows from Eqs. (32), (33), and (38). The only difference between schemes and their associated beamlines came as different numerical factors in front of the scaling. This scaling indicates very rapid increase of the ISR-induced debunching effect when either the beam energy or the dipole bend angle increases. As a result, the proposed XFEL seeding schemes should utilize elements with small bend angles. The maximum bend angle can be estimated from the condition that the ISR-induced diffusion does not reduce the amplitude of harmonic current by more than a factor of 2. The rapid scaling of the attenuation versus bend angle indicates that different beamlines having different numerical factors for attenuation scaling result in similar critical angles for bends. From this perspective, a significant complication of the beamline optics to reduce ISR-induced debunching does not seem practical.

6. Acknowledgements

Authors are thankful to D. V. Mozyrsky for useful discussions. This work is supported by the U.S. Department of Energy through the LANL/LDRD program.

Appendix A. Calculation of harmonic current reduction in chicane

In this Appendix we present the algorithm for calculating the attenuation of the harmonic current in a chicane which transforms an initial beam modulation into longitudinal bunching. However, the same algorithm can be used to calculate the smearing of an arbitrary short-scale modulation in an arbitrary beamline.

The Degradation of the harmonic current can be described with the Fokker-Planck equation (29) which describes beam energy diffusion coupled with the 6D phase space transport. In Secs. 3.3 and 3.4 we assumed phase space variables to be canonical conjugate. However, the variables do not have to be canonical in order to correctly describe the beam transport since our analysis of ISR effect did not use the condition for conjugance of variables. Therefore, one can choose conventional set of variables, i.e. $\zeta(s) = (x, x', y, y', c\Delta t, \Delta \gamma/\gamma)$, where x' and y' are the particle angles in respect to reference trajectory.

We describe the chicane as two doglegs separated by a drift space as illustrated in Fig. A.3. To simplify our analysis, we consider hard edge bends. Then the particle motion in the orthogonal y-plane is decoupled from the motion in the other phase space planes and it is represented by a simple drift. Therefore, energy diffusion affects motion only in x and z phase space planes and the system dynamics can be adequately described by 4D phase space.

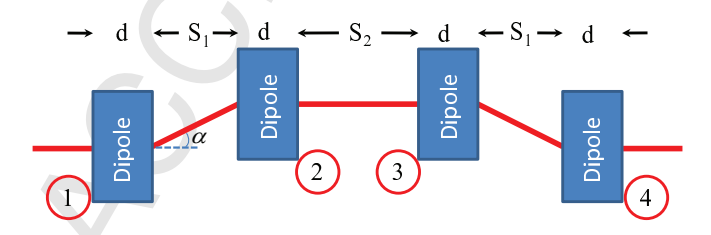


Figure A.3: (Color online) Schematic of a chicane.

The transform matrix of the chicane shown in Fig. A.3 is equal to

$$R_{\text{chicane}} = R_{\text{flip}} R_{\text{dogleg}} R_{\text{flip}} R_{\text{drift}} R_{\text{dogleg}} = \begin{bmatrix} 1 & 2L + S_2 & 0 & 0 \\ 0 & 1 & 0 & 0 \\ 0 & 0 & 1 & 2\xi \\ 0 & 0 & 0 & 1 \end{bmatrix}, \tag{A.1}$$

$$R_{\text{drift}} = \begin{bmatrix} 1 & S_2 & 0 & 0 \\ 0 & 1 & 0 & 0 \\ 0 & 0 & 1 & 0 \\ 0 & 0 & 0 & 1 \end{bmatrix}, R_{\text{flip}} = \begin{bmatrix} -1 & 0 & 0 & 0 \\ 0 & -1 & 0 & 0 \\ 0 & 0 & 1 & 0 \\ 0 & 0 & 0 & 1 \end{bmatrix},$$

$$R_{\text{dogleg}} = \begin{bmatrix} 1 & L & 0 & \eta \\ 0 & 1 & 0 & 0 \\ 0 & \eta & 1 & \xi \\ 0 & 0 & 0 & 1 \end{bmatrix}.$$
(A.2)

Here the dogleg parameters can be found in the ultra relativistic limit as

$$L = \frac{2d\cos\alpha + S_1}{\cos^2\alpha},$$

$$\eta = \frac{S_1 + 2d\cos\alpha - (2d + S_1)\cos^2\alpha}{\sin\alpha\cos^2\alpha},$$

$$\xi = \frac{2d\sin\alpha\cos\alpha - 2d\alpha\cos^2\alpha + S_1\sin^3\alpha}{\sin\alpha\cos^2\alpha},$$
(A.3)
(A.4)

$$\eta = \frac{S_1 + 2d\cos\alpha - (2d + S_1)\cos^2\alpha}{\sin\alpha\cos^2\alpha},\tag{A.4}$$

$$\xi = \frac{2d\sin\alpha\cos\alpha - 2d\alpha\cos^2\alpha + S_1\sin^3\alpha}{\sin\alpha\cos^2\alpha},$$
 (A.5)

where α is the bend angle of the dipole with parallel pole faces, d is the dipole length, S_1 is the distance between bends in each dogleg, and S_2 is the distance between the two doglegs [17].

Finding the attenuation of the harmonic current requires knowledge of the modulation wavevector inside each bend. First we find the modulation wavevector at the edge of each dipole using Eq. (28) which describes its transform along the beamline. We consider the output modulation of the beam to be longitudinal bunching, $\mathbf{k}(4) = 2\pi/\lambda \times [0,0,1,0]^T$. Then the modulation wavevector at positions 1, 2, and 3 along the beamline can be found as

$$\mathbf{k}(1) = R_{\text{chicane}}^T \mathbf{k}(4) = 2\pi/\lambda [0, 0, 1, 2\xi]^T,$$
 (A.6)

$$\mathbf{k}(2) = R_{\text{dogleg}}^{-T} \mathbf{k}(1) = 2\pi/\lambda [0, -\eta, 1, \xi]^{T},$$

$$\mathbf{k}(3) = R_{\text{drift}}^{-T} \mathbf{k}(2) = 2\pi/\lambda [0, -\eta, 1, \xi]^{T},$$
(A.7)
(A.8)

$$\mathbf{k}(3) = R_{\text{drift}}^{-T} \mathbf{k}(2) = 2\pi/\lambda [0, -\eta, 1, \xi]^T,$$
 (A.8)

$$\mathbf{k}(4) = 2\pi/\lambda [0, 0, 1, 0]^{T}. \tag{A.9}$$

The wavenumber of modulation inside each bend can be found using the transform matrix of the bend from its edge to some intermediate plane

$$R_{\theta} = \begin{bmatrix} \cos \theta & \rho \sin \theta & 0 & \rho (1 - \cos \theta) \\ -\sin \theta / \rho & \cos \theta & 0 & \sin \theta \\ -\sin \theta & \rho (\cos \theta - 1) & 1 & \rho (\sin \theta - \theta) \\ 0 & 0 & 0 & 1 \end{bmatrix}, \tag{A.10}$$

where the intermediate angle inside the bend is defined as θ to distinguish it from the overall bend angle α of the dipoles. Then the modulation wavevector in each bend

$$\mathbf{k}^{(1)}(\theta) = R_{\theta}^{-T}\mathbf{k}(1),\tag{A.11}$$

$$\mathbf{k}^{(2)}(\alpha - \theta) = (R_{\text{flip}}R_{\theta}R_{\text{flip}})^T\mathbf{k}(2),\tag{A.12}$$

$$\mathbf{k}^{(3)}(\theta) = (R_{\text{flip}} R_{\theta} R_{\text{flip}})^{-T} \mathbf{k}(3), \tag{A.13}$$

$$\mathbf{k}^{(4)}(\alpha - \theta) = R_{\theta}^T \mathbf{k}(4). \tag{A.14}$$

Using Eq. (27) in the limit of $k_E\hbar\omega_c\ll 1$ one can find the attenuation of the harmonic current in each dipole. Note that we use $\Delta \gamma / \gamma$ instead of ΔE as an independent energy variable and the bend angle θ instead of s as the path length variable in the Fokker-Planck equation. This choice of variables changes the diffusion coefficient to $D_{\theta} = \rho/(\gamma mc^2)^2 D$ and the energy modulation wavenumber to $k_{\Delta\gamma/\gamma} = \gamma mc^2 k_E$. The overall reduction in the modulation amplitude is equal to the product of attenuation factors in each element. Calculating the integrals in the limit of small bend angles, $\alpha \ll$ 1, one obtains the following expression for the attenuation of the harmonic current in the chicane

$$A_{\text{chicane}} = \exp \left\{ -\sum_{i=1}^{4} \int_{0}^{\alpha} \left(k_{\Delta\gamma/\gamma}^{(i)}(\theta) \right)^{2} D_{\theta} d\theta \right\} \approx$$

$$\approx \exp \left\{ -6700 \frac{\alpha^{7} [\text{deg}]}{\lambda^{2} [\mathring{A}]} \left(\frac{E}{10 GeV} \right)^{5} \times \right\}$$

$$\times \left[\left(\frac{R_{56}}{\rho \alpha^3} + 0.072 \right)^2 + 0.022 \right] \right\},$$
 (A.15)

where $R_{56} \equiv 2\xi$ is the chicane strength.

References

- A. M. Kondratenko and E. L. Saldin, Generation of coherent radiation by a relativistic electron beam in an ondulator, Part. Accel. 10 (1980), 207.
- [2] J. Feldhaus, E. L. Saldin, J. R. Schneider, E. A. Schneidmiller, and M. V. Yurkov, Possible application of X-ray optical elements for reducing the spectral bandwidth of an X-ray SASE FEL, Opt. Comm. 140 (1997), 341.
- [3] G. Geloni, V. Kocharyan, and E. Saldin, A novel self-seeding scheme for hard X-ray FELs, J. Modern Optics 58 (2011), 1391.
- [4] L. H. Yu, Generation of intense uv radiation by subharmonically seeded single-pass free-electron lasers, Phys. Rev. A 44 (1991), 5178.
- [5] G. Stupakov, Using the Beam-Echo Effect for Generation of Short-Wavelength Radiation, Phys. Rev. Lett. 102 (2009), 074801; D. Xiang and G. Stupakov, Echo-enabled harmonic generation free electron laser, Phys. Rev. ST Accel. Beams 12 (2009), 030702.
- [6] S. G. Biedrona, S. V. Miltona, and H. P. Freund, Modular approach to achieving the next-generation X-ray light source, Nucl. Instr. and Meth. A 475 (2001), 401.
- [7] B. Jiang, J. G. Power, R. Lindberg, W. Liu, and W. Gai, Emittance-Exchange-Based High Harmonic Generation Scheme for a Short-Wavelength Free Electron Laser, Phys. Rev. Lett. 106 (2011), 114801.
- [8] D. Ratner, A. Chao, and Z. Huang, Two-chicane compressed harmonic generation of soft x rays, Phys. Rev. ST Accel. Beams **14** (2011), 020701.
- [9] V. N. Litvinenko, et al., Optics-free X-ray FEL oscillator, Proc.2010 FLS Workshop, Menlo Park, CA, United States.

- [10] M. Sands, Synchrotron Oscillations Induced by Radiation Fluctuations, Phys. Rev. **97** (1955), 470.
- [11] N. A. Yampolsky, Dynamics of modulated beams in spectral domain, submitted to NIM A.
- [12] J. D. Jackson, Classical Electrodynamics, 3rd Edition, John Wiley & Son, Inc., 1999.
- [13] E. L. Saldin, E. A. Schneidmiller, and M. V. Yurkov, Calculation of energy diffusion in an electron beam due to quantum fluctuations of undulator radiation, Nucl. Instr. and Meth. A 381 (1996), 545.
- [14] M. Cornacchia and P. Emma, Transverse to longitudinal emittance exchange, Phys. Rev. ST Accel. Beams 5 (2002), 084001; Y.-E. Sun, P. Piot, A. Johnson, A. H. Lumpkin, T. J. Maxwell, J. Ruan, and R. Thurman-Keup, Tunable Subpicosecond Electron-Bunch-Train Generation Using a Transverse-To-Longitudinal Phase-Space Exchange Technique, Phys. Rev. Lett. 105 (2010), 234801.
- [15] B. E. Carlsten et al., New X-ray free-electron laser architecture for generating high fluxes of longitudinally coherent 50keV photons, J. Modern Optics 58 (2011), 1374;
- [16] B E. Carlsten, K. A. Bishofberger, S. J. Russell, and N. A. Yampolsky, Using an emittance exchanger as a bunch compressor, Phys. Rev. ST Accel. Beams 14 (2011), 084403.
- [17] P. Piot, Y.-E. Sun, J. G. Power, and M. Rihaoui, Generation of relativistic electron bunches with arbitrary current distribution via transverse-to-longitudinal phase space exchange, Phys. Rev. ST Accel. Beams 14 (2011), 022801;